JOURNAL OF SOLID STATE CHEMISTRY 110, 264–269 (1994)

An X-Ray Study of the Polymorphism in Thallium Monosulfide: The Structure of Two Tetragonal Forms

S. Kashida and K. Nakamura

Department of Physics, Niigata University, Ikarashi, Niigata, 950-21, Japan

Received May 4, 1993; in revised form September 7, 1993; accepted September 15, 1993

Thallium monosulfide is a mixed valence compound, as represented by the formula $Tl^{I}Tl^{III}S_2$. Two different structures with tetragonal symmetry are identified in TlS. The first is space group $I4/mcm$: $a = b = 7.785(2)$, $c = 6.802(2)$ Å, and $Z = 8$ (the TlSe type). The structure is characterized by chains formed of edge-connected $Tl^{III}S_4$ tetrahedra. Monovalent Tl^{I} ions are located between the chains and have eightfold antiprismatic coordination of the sulfur ions. The second is space group $P4_12_12$: $a = b = 7.803(9)$, $c = 29.55(2)$ Å, and $Z = 32$. The structure is characterized by layers formed of corner-connected $Tl^{III}S_4$ tetrahedra. Monovalent Tl^{I} ions are located between the layers and have sevenfold capped trigonal coordination of the sulfur ions. © 1994 Academic Press, Inc.

1. INTRODUCTION

The ternary compounds of thallium, such as $TlGaSe_2$ and $TlInS_2$, are semiconductors with the general formula $Tl^{I}M^{III}X_2$, where M = In or Ga and X = S, Se, or Te. These compounds have excited practical interest as optoelectronic devices. Until now, three structure types have been reported for this thallium chalcogenide series: type I, tetragonal TlSe structure (1); type II, monoclinic $TlGaSe_2$ structure (2); type III, tetragonal layer-type structure (3). Detailed crystal data, however, are available only for $TlGaSe_2$ (2). For other compounds of this series, controversial results have been reported, such as the unit cell parameters and the space groups; see Henkel *et al.* (3). As will be clarified later, some of the confusion may be ascribed to the polymorphism inherent in the ternary thallium compounds.

Thallium monosulfide can also be classified in this family. It contains thallium atoms with different valences, represented as $Tl^{I}Tl^{III}S_2$ (hereafter, in order to distinguish Tl atoms with the nominal valences +1 and +3, we use Roman numerals). The electrical properties and infrared spectra of TlS have been reported by several authors (4–6). Due to difficulties in obtaining single crystal samples, however, little is known about its other properties. Powder X-ray diffraction data were first reported by Hahn and Klinger (7), who showed that TlS is isostructural to TlSe (type I). In a later study, Scatturin and Frasson (8) reported the cell constants and the atomic positions, but single crystal diffraction data have not been given yet.

In a recent X-ray study, we found that TlS also crystallizes in a monoclinic structure (9) (type II, see Fig. 1). We also found another tetragonal structure. It has a layer structure similar to that of the monoclinic type, but belongs to the real tetragonal space group (type III). Only the existence of this type III, called "tetragonal monoclinic" (3), is reported in the ternary thallium chalcogenides. In this report, detailed structural data for these two tetragonal structures (type I and type III) will be presented.

2. EXPERIMENTAL

Single crystal samples of TlS were grown from melts. Details of the sample preparation were reported elsewhere (9). Depending upon the cooling rate, two differently shaped TlS crystals were obtained: when the melt was cooled very slowly, needle-like crystals were grown, whereas when it was cooled rather rapidly, plate-like crystals were grown (an amorphous sample was obtained when it was quenched).

The crystal symmetry and approximate lattice constants were determined using precession photographs. The needle-like crystal was assigned as tetragonal with space group $I4/mcm$, $I\bar{4}c2$, or $I4cm$ (type I). Two different structures were identified for the plate-like samples; one is monoclinic with space group $C2$, Cm, or $C2/m$ (type II); and the other is tetragonal with space group $P4_12_12$ or $P4_32_12$ (type III). See Fig. 1.

The polymorphic types II and III are obtained by cleavage of the same type of plate-like crystals. In our experiment, they grew congruently. From the morphological features, it was not possible to distinguish types II and III, but single crystal X-ray photographs can easily separate these two polymorphs.

The detailed structure of type II is presented elsewhere (10) and not reproduced here. This monoclinic crystal of TlS has a structure with fourfold modulation along the c

0022-4596/94 $6.00

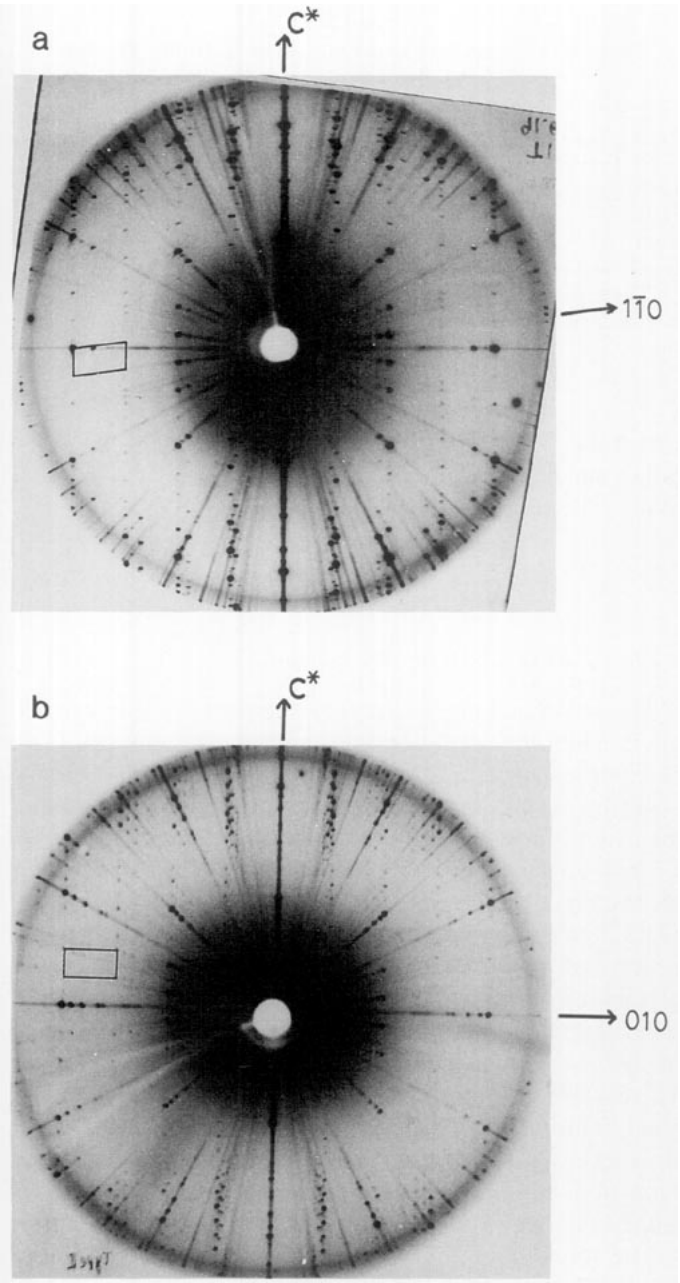

FIG. 1. Precession photographs of the layer-type TlS, taken at room temperature. (a) The [110] zone of the monoclinic type II. (b) The [010] zone of the tetragonal type III. The inserted quadrangles show the unit areas for the sublattice structures. Note that the extra reflections are observed along the c* axis (a) at ¼, and (b) at ½.

axis. The subcell or "average" structure of type II is very close to that reported for $TlGaSe_2$ (2); see Fig. 2.

For the intensity measurements, samples were cleaved from crystalline blocks. The type III crystals were easily cleaved along the (001) plane, while along other directions the cleavage was not distinct. The cleavage planes of the type III crystals are (001), (100), and (010). Type I crystals also show cleavage along the (110) plane. The cleaved samples were carefully selected using the precession photographs, since in most cases the plate-like crystals were heavily twinned and furthermore are often composite crystals of types II and III. Unfortunately, the untwinned crystals thus obtained had rather large dimensions for the intensity measurements. Since the crystals are very sensitive to mechanical strains, they were not further divided or ground into spheres.

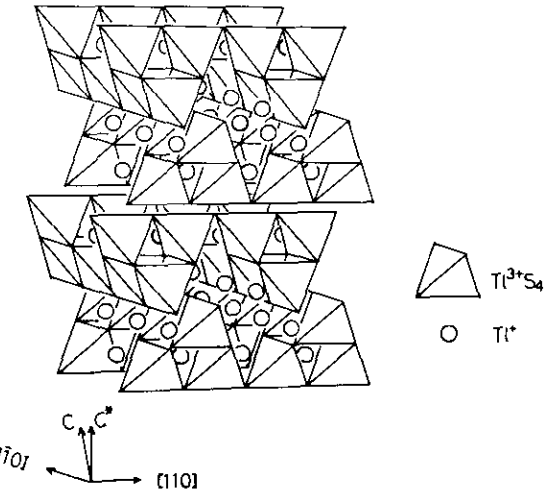

FIG. 2. Schematic drawing of the "average" structure of type II (the monoclinic $TlGaSe_2$ type). This structure is characterized by layers composed of corner-connected $Tl^{III}S_4$ tetrahedra. The upper and lower edges of the tetrahedra are linked along the [110] and [1$\bar{1}$0] axes. Tl^I ions are located along channels between the layers.

The diffraction data were collected on a Huber four-circle diffractometer. Graphite-monochromated Mo$K\alpha$ radiation (0.7107 Å) was used. Three standard reflections were monitored every 100 reflections in intensity measurements. No significant variation was detected in either case. The intensity data were corrected for the Lp factors. Since the samples had relatively large sizes, the data were corrected for absorption by numerical integration. Table 1 summarizes the relevant crystal data, data collection, and refinement information.

3. STRUCTURE DETERMINATION

The structures were solved by the heavy-atom method.[1] The refinements were performed using the full-matrix

[1] A list of structure factors, anisotropic thermal parameters, bond distances, and bond angles have been deposited with the National Auxiliary Publication Service. See NAPS document No. 05057 for 43 pages of supplementary material from ASIS/NAPS, Microfiche Publications, P. O. Box 3513, Grand Central Station, New York, NY 10163. Remit in advance $4.00 for microfiche copy or for photocopy, $7.75 up to 20 pages plus $.30 for each additional page. All orders must be prepaid. Institutions and Organizations may order by purchase order. However, there is a billing and handling charge for this service of $15. Foreign orders add $4.50 for postage and handling, for the first 20 pages, and $1.00 for additional 10 pages of material, $1.50 for postage of any microfiche orders.

TABLE 1

	(a) Crystal data	
Type	I tetragonal chain type	III tetragonal layer type
Space group	$I4/mcm$	$P4_12_12$
Lattice parameters (Å)	a = 7.785(2) b = a c = 6.802(2)	a = 7.803(9) b = a c = 29.55(2)
Z	8	32
Volume (Å^3)	412.2	1799.0
D-calc (Mg/m^3)	7.62	6.98
Absorption coefficient (1/mm)	79.64	72.95
Crystal size (mm)	.19 × .10 × .30	.38 × .26 × .10
T_{max}; T_{min} ($\times 10^{-3}$) (transmission factors)	2.8; 1.3	4.0; 1.4
	(b) Data collection	
Measurement temperature	298 K	295 K
Scan mode	$\omega/2\theta$	$\omega/2\theta$
2θ max (deg)	60	60
Range in indices		
h	0–10	0–10
k	0–10	0–10
l	0– 9	0–38
No. of independent reflections measured	201	1336
R_{INT}	0.098	0.100
	(c) Refinement	
No. of reflections used in refinement	136 ($I > \sigma(I)$)	578 ($I > 3\sigma(I)$)
No. of parameters refined	10	75
R	0.041	0.072
Maximum (shift/e.s.d.)	0.03	0.25
$\Delta\rho_{max}$ and $\Delta\rho_{min}$(e/Å^3)	+4 −8	+4 −4

least-squares program "RADIEL" (11). The function minimized was $\Sigma\, w(|F_o| - |F_c|)^2$, where w was set to 1 for all reflections. The atomic scattering factors (neutral atoms) and the anomalous dispersion terms were taken from the International Tables for X-Ray Crystallography (12).

The positions of the Tl atoms were deduced from Patterson maps, and those of the sulfur atoms were deduced from subsequent Fourier syntheses. For type I, the refinement of atomic positions showed that the correct space group is $I4/mcm$. The final R factor was 0.041. For type III, the space group compatible with the observed extinction rule was $P4_12_12$ or $P4_32_12$. The final R factor for space group $P4_12_12$ was 0.072 with anisotropic thermal parameters. It was also 0.072 for space group $P4_32_12$, where the coordinates were inverted. The quality of the present diffraction data was not good enough to select the correct space group. The calculated difference between the structure factors of the Bijvoet pairs was also rather small (below about 2%). Therefore, we have tentatively chosen the former space group $P4_12_12$.

TABLE 2
Positional Parameters and Equivalent Isotropic Thermal Parameters for Type I

Atom	x	y	z	U (eq)[a]
Tl(1)^1	0.0	0.0	0.25	0.034(2)
Tl(2)^3	0.0	0.5	0.25	0.019(1)
S (1)	0.1721(9)	0.6721(9)	0.0	0.014(3)

[a] The superscript in the first column represents the nominal atomic valence, and $U(\text{eq}) = \frac{1}{3}(U_{11} + U_{22} + U_{33})$. The esd's are given in parentheses.

4. DESCRIPTION OF THE STRUCTURE AND DISCUSSION

4.1 Type I (Tetragonal TlSe Structure)

The positional and thermal parameters are given in Table 2. The bond distances and angles are given in Table 3. The present values, such as the cell constants, atomic positions, and the Tl–S atomic distances, are in fair agreement with those given by Scatturin and Frasson (8).

Figure 3 shows the structure of type I. This structure is characterized by linear chains formed of edge-connected $Tl^{III}S_4$ tetrahedra; monovalent Tl^I ions are located between the negatively charged chains. The Tl^{III} ions are assumed to form sp^3-type bonding. The observed Tl^{III}–S bond distance of 2.54 Å is in fair agreement with the sum of the covalent radii of Tl (1.58 Å) and S (1.07 Å) (13). The S–Tl^{III}–S angles are 117° and 96°, deviating from the ideal value of 109.5°; the tetrahedra are elongated along the c axis. This distortion is attributed to the electrostatic repulsion between the thallium ions. The Tl^{III}–S–Tl^{III} angle is about 84°.

The monovalent Tl^I ion has eightfold coordination of the sulfur ions. The average value of the Tl^I–S distance (3.35 Å) is in fair agreement with the sum of the ionic radii of Tl^{1+} (1.47 Å) and S^{2-} (1.84 Å) (14). The Tl–Tl

TABLE 3
Selected Bond Distances (Å) and Angles (°) in Type I

Tl(1)^1–S (1)	3.347(6)	Tl(2)^3–S (1)	2.546(5)
Tl(1)^1–Tl(2)^3	3.892(1)	Tl(2)^3–Tl(2)^3	3.401(1)
Tl(1)^1–Tl(1)^1	3.401(1)	Tl(2)^3–Tl(1)^1	3.892(1)
S (1) –S (1)	3.790(9)		
S (1)–Tl(2)^3–S(1)	116.5(2)		
S (1)–Tl(2)^3–S(1)	96.2(2)		

Note. The esd's are given in parentheses. The superscript represents the nominal atomic valence.

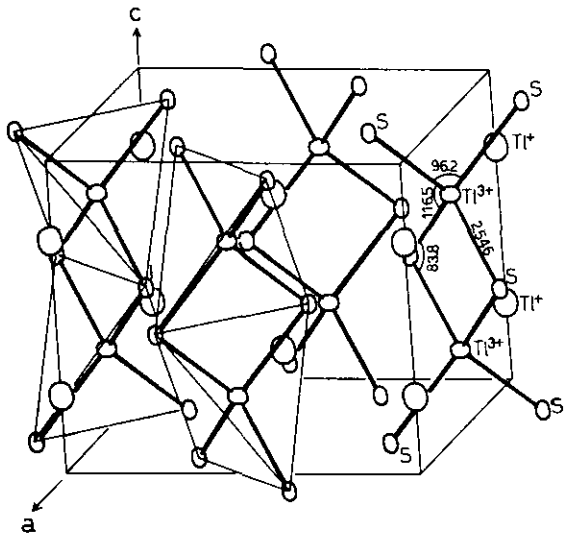

FIG. 3. Structure of TlS type I (tetragonal TlSe type). The thermal ellipsoids are for 50% probability. For clarity, some of the $Tl^{III}S_4$ tetrahedra are drawn with thin solid lines.

distance of 3.40 Å can be compared with the value of 3.35 Å for metallic thallium. The monovalent Tl^{I} ion has relatively large thermal parameters compared with those of the Tl^{III} ion (cf. Table 2).

The TlSe type (type I) has a density larger than that of the type III (about 9%; see Table 1). The TlSe structure is considered to be a modification of the CsCl type. In a recent high-pressure experiment, Demishev *et al.* (15) reported that above 25 GPa, TlS changes to the CsCl structure (a = 3.202 Å). In this CsCl structure, the Tl atoms are expected to become divalent.

A final difference Fourier map shows residual peaks around the Tl ions. Positive peaks (+4 e/Å^3) are found along the ⟨110⟩ axis and negative peaks (−8 e/Å^3) along the ⟨100⟩ direction connecting the nearest-neighbor Tl sites. Since we have used a nonspherical sample having large absorption, the origin of these residual peaks will be ascribed to incompleteness of the absorption correction. However, parts of the origin may be ascribed to anharmonic motions of the Tl^{I} ion.

4.2 Type III (Tetragonal Layer Structure)

The atomic coordinates and thermal parameters are given in Table 4, and the bond distances and angles are listed in Table 5. This structure is a modification of the monoclinic $TlGaSe_2$ type (2); see Fig. 4. The Tl^{III} ion has fourfold coordination of the sulfur ions. The average Tl^{III}–S distance of 2.50 Å is nearly the same as that in type I. The S–Tl^{III}–S bond angles deviate from the ideal tetrahedral value of 109.5° and range from 100° to 120°. The distortion of the $Tl^{III}S_4$ tetrahedra, however, is not so large as in type I. The Tl^{III}–S–Tl^{III} angles are in the range from 99° to 110°.

TABLE 4
Positional Parameters and Equivalent Isotropic (Tl) or Isotropic (S) Thermal Parameters for Type III

Atom	x	y	z	U(eq)
$Tl(1)^3$	0.6217(5)	0.3699(15)	0.476(1)	0.023(1)
$Tl(2)^3$	0.1273(5)	0.3735(16)	0.0518(1)	0.023(2)
$Tl(3)^1$	0.8708(8)	0.9014(18)	0.0665(8)	0.048(5)
$Tl(4)^1$	0.3774(8)	0.9021(11)	0.0648(1)	0.034(3)
S (1)	0.641(9)	0.641(9)	0.0	0.041(11)
S (2)	0.112(15)	0.112(15)	0.0	0.036(10)
S (3)	0.122(8)	0.637(5)	0.0058(8)	0.029(6)
S (4)	0.377(5)	0.332(7)	0.1011(10)	0.038(7)
S (5)	0.871(4)	0.320(3)	0.1006(8)	0.035(7)

Note. The superscript in the first column represents the nominal atomic valence, and $U = \frac{1}{3}(U_{11} + U_{22} + U_{33})$. The esd's are given in parentheses.

The Tl^{I} ion has a trigonal prismatic coordination of the sulfur ions. The average Tl^{I}–S distance of 3.31 Å is nearly the same as that in type I. The average Tl^{I}–Tl^{I} distance is 3.93 Å and is longer than that of type I (3.4 Å). The monovalent Tl(4) ion and the apical sulfur ions (S(4) and S(5)) are displaced normal to the channel direction in reverse (see also the arrows in Fig. 5). Thus, the Tl^{I} ion is displaced from the center of the trigonal prism and has sevenfold coordination of the sulfur ions (capped trigonal

TABLE 5
Selected Bond Distances (Å) and Angles (deg) in Type III

$Tl(1)^3$–S (1)	2.542(10)	$Tl(2)^3$–S (2)	2.553(10)
$Tl(1)^3$–S (3)	2.500(9)	$Tl(2)^3$–S (3)	2.465(10)
$Tl(1)^3$–S (4)	2.494(4)	$Tl(2)^3$–S (4)	2.46(4)
$Tl(1)^3$–S (5)	2.53(4)	$Tl(2)^3$–S (5)	2.50(4)
$Tl(1)^3$–$Tl(2)^3$	3.859(4)	$Tl(2)^3$–$Tl(1)^3$	3.859(4)
$Tl(1)^3$–$Tl(3)^1$	4.03(3)	$Tl(2)^3$–$Tl(4)^1$	3.853(3)
$Tl(3)^1$–S (1)	3.349(17)	$Tl(4)^1$–S (1)	3.462(6)
$Tl(3)^1$–S (2)	3.177(17)	$Tl(4)^1$–S (2)	3.252(6)
$Tl(3)^1$–S (3)	3.36(4)	$Tl(4)^1$–S (3)	3.35(4)
$Tl(3)^1$–S (3′)	3.29(2)	$Tl(4)^1$–S (3′)	3.364(6)
$Tl(3)^1$–S (4)	3.18(2)	$Tl(4)^1$–S (4′)	3.53(3)
$Tl(3)^1$–S (5′)	3.42(3)	$Tl(4)^1$–S (4)	3.240(5)
$Tl(3)^1$–S (5)	3.16(2)	$Tl(4)^1$–S (5)	3.254(5)
$Tl(3)^1$–$Tl(1)^3$	4.03(3)	$Tl(4)^1$–$Tl(1)^3$	3.964(5)
$Tl(3)^1$–$Tl(4)^1$	3.953(9)	$Tl(4)^1$–$Tl(2)^3$	3.853(3)
$Tl(3)^1$–$Tl(4')^1$	3.850(6)	$Tl(4)^1$–$Tl(2')^3$	3.965(3)
S(1)–$Tl(1)^3$–S(3) 107(2)		S(2)–$Tl(2)^3$–S(3) 110(2)	
S(1)–$Tl(1)^3$–S(4) 120(2)		S(2)–$Tl(2)^3$–S(4) 107(2)	
S(1)–$Tl(1)^3$–S(5) 115(2)		S(2)–$Tl(2)^3$–S(5) 100(2)	
S(3)–$Tl(1)^3$–S(4) 110(1)		S(3)–$Tl(2)^3$–S(4) 117(1)	
S(3)–$Tl(1)^3$–S(5) 104(1)		S(3)–$Tl(2)^3$–S(5) 116(1)	
S(4)–$Tl(1)^3$–S(5) 100(1)		S(4)–$Tl(2)^3$–S(5) 106(1)	

Note. The superscript on the right-hand side represents atomic valence. The esd's are given in parentheses.

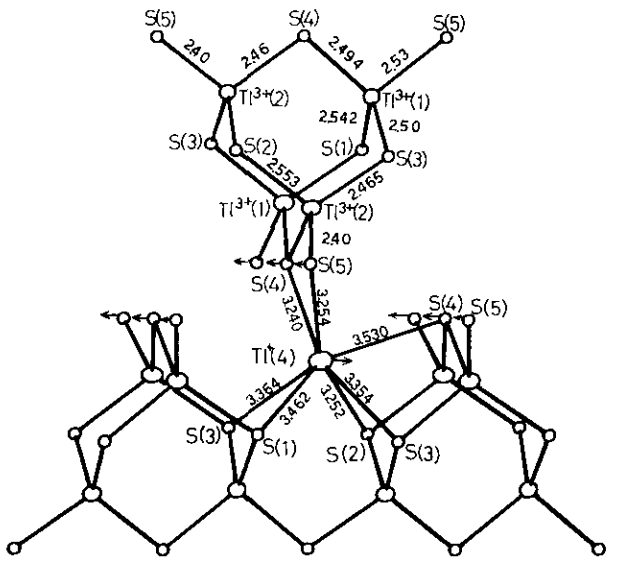

FIG. 4. Structure of TlS type III (tetragonal layer type). View along the channel between the succeeding layers. The thermal ellipsoids are for 50% probability. For clarity only two layers are shown. The Tl^{III} ion is coordinated by four sulfur ions, whereas the Tl^{I} ion is coordinated by seven sulfur ions. Note that the Tl(4) ion and the apical S(4), S(5) ions move in reverse direction, as shown by arrows.

coordination). In the basic $TlGaSe_2$ structure (2), the Tl^{I} ion is located in the middle of the trigonal prism. However, analysis of the modulated structure of type II (10) showed that the local coordinations of Tl^{I} ions are also distorted, as shown in Fig. 5.

This distortion may be attributed to the stereochemical instability of the $6s^2$ lone pair discussed by Orgel (16, 17). The idea is that the distortion around the Tl^{I} ion would cause Tl $6p$ orbitals to mix into the filled $6s$ level and lower the electronic energy. Along this line, Yee and Albright discussed the bonding in $TlGaSe_2$ using the extended Hückel Hamiltonian (18). Assuming a $Tl^{I}Se_6$ molecule in a trigonal prismatic coordination, they showed that the Tl^{I} ion would move along the channel direction and have three shorter and three longer chalcogen coordinations. It is, however, not consistent with the experimental results. We have followed their calculations and found that when two chalcogen ions are added in a bicapped trigonal coordination, the Tl ion would move normal to the channel direction and have sevenfold coordination of the chalcogen ions. However, the distortion considered here is not of the bending type but rather of the stretching type. A simple extended Hückel theory may not be suitable for the present case, since it does not take into account the core electron repulsion and gives too short atomic distances. Therefore, a more elaborate theory which includes the core electron repulsion will be necessary to clarify the electronic origin of the distortion.

Last, we will discuss the stacking sequence of the layers in type III. Figure 5 shows the projection of the structure along the [010] and [100] axes. The Tl^{III}–S layers are represented by coupled triangles. The unit cell of the basic monoclinic $TlGaSe_2$ structure (the "average" structure of type II) is composed of two such layers (the dotted lines). As the dotted lines show, in type III, a $\frac{1}{2}$ slip is introduced along the channel directions every four layers. The unit cell relations between the type III and the basic monoclinic $TlGaSe_2$ cell are

$$\boldsymbol{a}_{tet} = \tfrac{1}{2}(\boldsymbol{a}_m + \boldsymbol{b}_m),\ \boldsymbol{b}_{tet} = \tfrac{1}{2}(\boldsymbol{a}_m - \boldsymbol{b}_m),$$
$$\text{and } c_{tet} = 2 \times c_m \sin\beta$$

(the subscripts tet and m mean the tetragonal and monoclinic, respectively).

A final difference Fourier synthesis showed additional peaks ($+4\ e/Å^3$) at positions midway between the Tl ions. Additional weak peaks were also observed at positions midway between the S ions. In the precession photographs, we have observed rather strong diffuse streaks along the c^* axis when the index h or k is odd. These extra electron densities are, therefore, attributed to the stacking faults. It is worth discussing this point more extensively. As is shown in Fig. 5, when the stacking

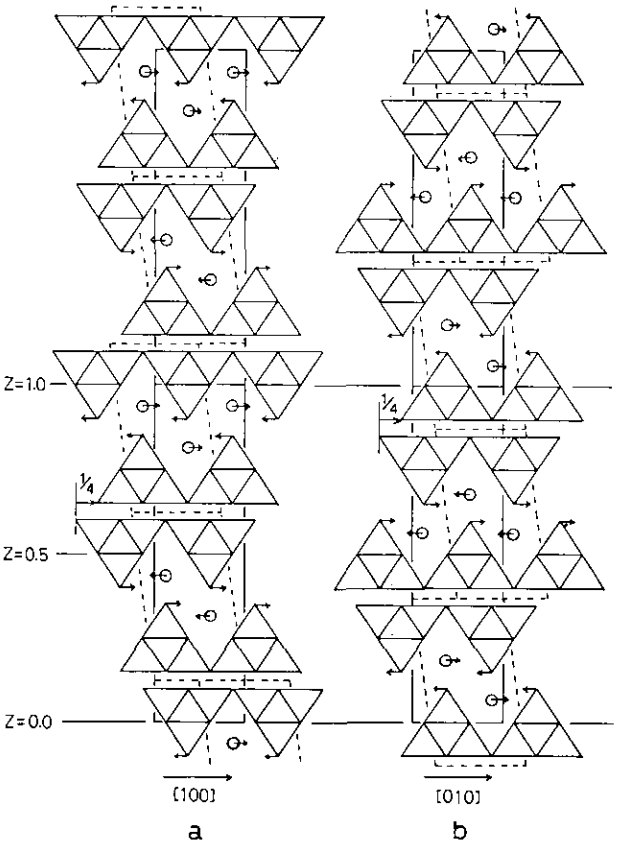

FIG. 5. Schematic representation of the layer stackings in type III: (a) projection along the [010] axis, (b) projection along the [100] axis. The triangles represent $Tl^{III}S_4$ tetrahedra. The dotted lines represent the basic $TlGaSe_2$ cell. The arrows represent relative displacements of atoms.

sequence is viewed along the channels of the Tl^{I} ions, the lower edge of the upper layer is just in the middle between the upper edges of the lower layer. In contrast, when viewed normal to the channel direction, the triangles in the upper succeeding subcell are displaced $\frac{1}{4}$ along the channel direction. In another version of the stacking, they are displaced $-\frac{1}{4}$ along this direction. From symmetry, this ambiguity arises along both the [100] and [010] axes. As a result, there are four stacking types. This ambiguity will be the origin of the stacking disorder and produces ghosts at positions midway between the settled atoms. The stacking faults are also observed in monoclinic type II (10), as already reported for $TlGaSe_2$ by Müller and Hahn (2) and McMorrow *et al.* (19).

ACKNOWLEDGMENTS

The authors thank Professor S. Katayama for helpful discussion. They also thank Mr. K. Yamamoto for his help in computation.

REFERENCES

1. J. A. A. Ketelaar, W. H. t'Hart, M. Moerel, and D. Polder, *Z. Kristallogr.* **101,** 396 (1939).
2. D. Müller and H. Hahn, *Z. Anorg. Allg. Chem.* **438,** 258 (1978).
3. W. Henkel, H. D. Hochheimer, C. Carlone, A. Werner, S. Ves, and H. G. v. Schnering, *Phys. Rev. B* **26,** 3211 (1982).
4. R. S. Itoga and C. R. Kannewurf, *J. Phys. Chem. Solids* **32,** 1099 (1971).
5. A. T. Nagat, *J. Phys.: Condens. Matter* **1,** 7921 (1989).
6. K. R. Allakhverdiev, M. A. Nizametdinova, E. Yu. Salaev, R. M. Sardarly, N. Yu. Safarov, E. A. Vinogradov, and G. N. Zhizhin, *Solid State Commun.* **36,** 527 (1980).
7. H. Hahn and W. Klinger, *Z. Anorg. Allg. Chem.* **260,** 110 (1949).
8. V. Scatturin and E. Frasson, *Ric. Sci.* **26,** 3382 (1956).
9. S. Kashida, K. Nakamura, and S. Katayama, *Solid State Commun.* **82,** 127 (1992).
10. K. Nakamura and S. Kashida, *J. Phys. Soc. Jpn.* **62,** 3135 (1993).
11. P. Coppens, T. N. Guru Row, P. Leung, E. D. Stevens, P. J. Becker, and Y. W. Yang, *Acta Crystallogr. Sect. A* **35,** 63 (1979).
12. "International Tables for X-Ray Crystallography," Vol. IV. Kynoch Press, Birmingham, 1974. (Present distributor Kluwer, Dordrecht.)
13. L. Pauling, "The Nature of the Chemical Bond." Cornell Univ. Press, Ithaca, New York, 1960.
14. "CRC Handbook of Chemistry and Physics," 69th ed. (R. C. Weast, M. J. Astle, and W. H. Beyer, Eds.), pp. F164. CRC Press Inc., Boca Raton, Florida, 1988.
15. G. B. Demishev, S. S. Kabalkina, and T. N. Kolobyanina, *Phys. Status Solidi A* **108,** 89 (1988).
16. L. E. Orgel, *J. Chem. Soc.* **4,** 3815 (1959).
17. H. D. Hochheimer, E. Gmelin, W. Bauhofer, Ch. v. Schnering-Schwarz, H. G. v. Schnering, J. Ihringer, and W. Appel, *Z. Phys. B: Condens. Matter* **73,** 257 (1988).
18. K. A. Yee and T. A. Albright, *J. Am. Chem. Soc.* **113,** 6474 (1991).
19. D. F. McMorrow, R. A. Cowley, P. D. Hatton, and J. Banys, *J. Phys.: Condens. Matter* **2,** 3699 (1990).